

The X-rays detecting system of the FAMU experiment for the measurement of the muon transfer rate to carbon

S. Monzani,^{a,b} A. Adamczak,^c D. Bakalov,^d G. Baldazzi,^{e,f} M. Baruzzo,^a R. Benocci,^{g,h} R. Bertoni,^g M. Bonesini,^{g,i} H. Cabrera,^{a,j} D. Cirrincione,^{a,b} M. Clemenza,^{g,i} L. Colace,^{k,l} M. Danailov,^{a,m} P. Danev,^d A. de Bari,^{n,o} E. Fasci,^p K. S. Gadedjisso-Tossou,^{a,j,q} L. Gianfrani,^p K. Ishida,^r A. Menegolli,^{n,o} E. Mocchiutti,^a L. Moretti,^p G. Morgante,^e C. Petroselli,^{s,g} C. Pizzolotto,^a A. Pullia,^{t,u} R. Ramponi,^{t,v} L. P. Rignanese,^e H. E. Roman,^{g,i} M. Rossella,^o R. Rossini,^{n,o} A. Sbrizzi,^e M. Stoilov,^d J. J. Suárez-Vargas,^a L. Tortora,^l E. Vallazza^g and A. Vacchi^{a,b,r}

^aSezione INFN di Trieste, via A. Valerio 2, Trieste, Italy

^bDipartimento di Scienze Matematiche, Informatiche e Fisiche, Università di Udine, via delle Scienze 206, Udine, Italy

^cInstitute of Nuclear Physics, Polish Academy of Sciences, Radzikowskiego 152, PL31342 Kraków, Poland

^dInstitute for Nuclear Research and Nuclear Energy, Bulgarian Academy of Sciences, blvd. Tsarigradsko ch. 72, Sofia 1784, Bulgaria

^eSezione INFN di Bologna, viale Berti Pichat 6/2, Bologna, Italy

^fDipartimento di Fisica ed Astronomia, Università di Bologna, via Irnerio 46, Bologna, Italy

^gSezione INFN di Milano Bicocca, Piazza della Scienza 3, Milano, Italy

^hDipartimento di Scienze dell'Ambiente e della Terra, Università di Milano Bicocca, Piazza della Scienza 1, Milano, Italy

ⁱDipartimento di Fisica G. Occhialini, Università di Milano Bicocca, Piazza della Scienza 3, Milano, Italy

^jThe Abdus Salam International Centre for Theoretical Physics, Strada Costiera 11, Trieste, Italy

^kSezione INFN di Roma Tre, Via della Vasca Navale 84, Roma, Italy

^lDipartimento di Ingegneria, Università degli Studi Roma Tre, Via V. Volterra 62, Roma, Italy

^mSincrotrone Elettra Trieste, SS14, km 163.5, Basovizza, Italy

ⁿDipartimento di Fisica, Università di Pavia, via A. Bassi 6, Pavia, Italy

^oSezione INFN di Pavia, Via A. Bassi 6, Pavia, Italy

^pSezione INFN di Napoli e Dipartimento di Matematica e Fisica, Università della Campania "Luigi Vanvitelli", Viale Lincoln 5, Caserta, Italy

^qLaboratoire de Physique des Composants à Semi-conducteurs (LPCS), Département de physique, Université de Lomé, Lomé, Togo

^r*Riken Nishina Center, RIKEN, 2-1 Hirosawa, Wako, Saitama 351-0198, Japan*

^s*Dipartimento di Fisica, Università degli Studi dell'Insubria, via Ravasi 2, Varese, Italy*

^t*Sezione INFN di Milano, via Celoria 16, Milano, Italy*

^u*Dipartimento di Fisica, Università degli Studi di Milano, via Celoria 16, Milano, Italy*

^v*INFN-CNR, Dipartimento di Fisica, Politecnico di Milano, piazza Leonardo da Vinci 32, Milano, Italy*

E-mail: Simone.Monzani@uniud.it

The FAMU experiment is based on spectroscopy experiment. It uses exotic atoms to measure the proton Zemach radius, a convolution of the electronic and magnetic charge distribution. Specifically, there exists a direct correlation between the Zemach radius of the proton and the hyperfine splitting (HFS) in the muonic hydrogen energy ground level (μp). It is therefore a complementary way to study the proton compared to electron scattering experiments. The FAMU experimental technique takes advantage of the fact that, for given hydrogen gas mixtures, muons pass from the μp to the heavier gas atoms at a rate that is dependent on the μp energy. This results in X-rays counting rate from the heavier muonic atoms deexcitation cascade that depends on the energy of the μp . A fast detection system and excellent energy resolution in the 20-400 keV range are needed for this high precision experiment. The $\text{LaBr}_3(\text{Ce})$ detectors are read by PMTs in this phase of the experiment. The behavior of the muon transfer rate from hydrogen to carbon has been evaluated using a detailed analysis of the performances of the detectors, which are presented below.

6th International Conference on Technology and Instrumentation in Particle Physics (TIPP2023)

4 - 8 Sep 2023

Cape Town, Western Cape, South Africa

1. Introduction

The technique that was employed to investigate the properties of the proton, achieving remarkable degrees of precision in recent years, was elastic scattering. Techniques that use laser spectroscopy to measure the Lamb shift or 1S HFS in muonic hydrogen are highly sensitive and they enable increased precision by providing a different measurement approach than using regular hydrogen. A laser pulse tuned at the HFS resonance will bring the muonic hydrogen system from a singlet state $F = 0$ to a triplet state $F = 1$. As the the HFS comes from the interaction between the magnetic moment of the muon and the proton [1], the magnetic structure of the proton becomes accessible. The FAMU experiment aims to measure the Zemach radius of the proton with a relative precision better than 1 %, this exploiting the transfer rate of muons from the μp to the appropriate high-Z element [2] selected by FAMU among oxygen, carbon and argon.

2. The experimental setup and method

The FAMU experiment is located at the RIKEN RAL facility [3] where a pulsed-muon beam with a repetition rate of 50 Hz (double pulse with a separation of 320 ns) is stopped in a target with a gas mixture made by a cryogenic aluminium vessel at a pressure of 30 bar and surrounded by seven X-rays detectors [4]. The present work shows the analysis of the 2016 data sample collected with a gas mixture made of hydrogen and CH_4 at a mass concentration of 0.3 % at 4 temperatures: 300 K, 270 K, 240 K and 197 K. Each measurement corresponding to different pressure conditions lasts for 4 hours. The lowest temperature is fixed to avoid the condensation temperature of CH_4 .

3. The $LaBr_3(Ce)$ scintillating crystal

The X-rays detecting system is composed by seven $LaBr_3(Ce)$ scintillating crystals, one inch thick inside a case with a $2.5 \times 2.5 \text{ cm}^2$ (diameter x thickness) cylindrical shape. The FAMU experiment requires a high energy resolution as multiple X-rays are generated from the interaction of muons with matter. The transfer mechanism from the muonic hydrogen to carbon occurs in hundreds of nanoseconds and the $LaBr_3(Ce)$ timing resolution up to 500 ps is sufficient for this scope. The duration of signals is small, ideal to avoid pile-up with good linearity in pulsed high rate conditions. Finally the X-rays emission by the target is isotropic and this type of detectors can cover a large solid angle showing also a good stability over time. Scintillation light signals are collected and amplified using Hamamatsu high speed photomultipliers (R11265U-200, Fig. 1).

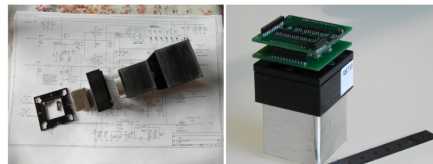


Figure 1: Left panel: disassembled detector, the circular $LaBr_3:Ce$ crystal, and the squared photomultipliers. Right panel: assembled detector with part of the electronic.

The energy and the time associated to each electrical pulse are extracted from the digitized waveforms recorded with a 500MHz CAEN V1730 digitizer.

4. The acquisition system

A 500 MHz digitizer recorded the output of the $\text{LaBr}_3(\text{Ce})$ detectors (Fig. 2) for about 10 μs after the trigger given by the accelerator. The long acquisition window is necessary as the energy spectrum of the X-rays and their time distribution are fundamental. The measurement of the transfer rate of muons from μp to carbon must be performed after the thermalization process of μp .

Therefore we define a prompt emission in the first 1000 ns during the two muon spills with X-rays from muons capture in elements in the target and from electron generated from the muon decay. A delayed emission follows with X-rays mostly coming from the muon transfer rate from the μp to carbon, where background is represented by X-rays from electrons from the muon decay and bremsstrahlung photons.

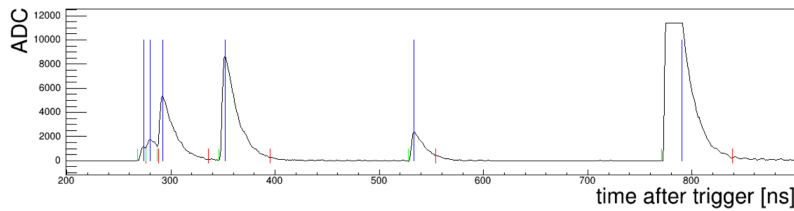


Figure 2: Waveforms from the digitizer of the $\text{LaBr}_3(\text{Ce})$ detectors after the subtraction of the baseline; vertical lines come from X-rays data reconstruction: green line start, blue line maximum, red line end.

The time and the height of the pulses are reconstructed and stored. The blue vertical lines in figure 2 identify the maximum of each reconstructed pulse. The first pulses are overlapped (pile up). Pile up is subtracted fitting the whole time-window with Landau functions to model pulse. The high energy pulse saturated and it is rejected through a cut on the baseline restoration. The starting time of a pulse is defined through the study of the derivative. Rise time is very fast and equal to 10 ns, while decay time is around 30 ns. Moreover baseline is constant in time and no relevant background neither undershoot are present.

5. Calibration and detector performances

The calibration consists in comparing the peaks of the prompt and the delayed spectra with the K-lines of the elements present in the target and in the gas mixture. Single or double gaussian fits are sufficiently accurate in most of the cases, a double gaussian fit with a functional model of the underlying background is less performing. The prompt X-rays lines come mostly from aluminium (65.8 keV, 88.8 keV, 346 keV) and nickel (107 keV, 309 keV), as it is in Fig. 3, left panel. Instead delayed X-rays are produced by the carbon atoms contained in the gas mixture, hundreds of ns after the arrival of the muon spills: K_α , K_β and K_γ lines at 75 KeV, 89 keV and 94 keV.

In the prompt region six emission lines (aluminium and nickel) are clearly visible confirming the high performances of the $\text{LaBr}_3(\text{Ce})$ detectors. Every single fit is converging in all the detectors. The increasing slope at low energy is due to the low-energy background.

A total of seven points coming from seven K-lines are considered for calibration. The K_β and K_γ lines of carbon are excluded from the calibration fit because they are not resolved.

The energy calibration is done by fitting with a second order polynomial as it is in Fig. 3, right

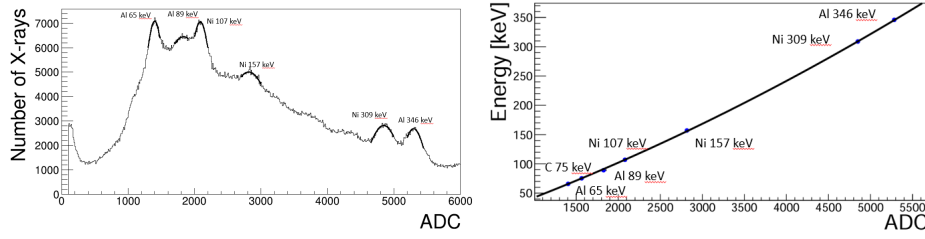


Figure 3: Prompt energy spectra measured with one $\text{LaBr}_3(\text{Ce})$ detector (left); calibration curve of one $\text{LaBr}_3(\text{Ce})$ detector, the error bar is included in the marker size and the coefficients of the polynomial fit to the data points in increasing order are -11.2 ± 1.9 , $(5.02 \pm 0.14) \times 10^{-2}$, $(3.4 \pm 0.2) \times 10^{-6}$ (right).

panel, with a higher density of points at a low energy in the energy region corresponding to the carbon K-lines. The horizontal error bar is estimated by varying the fitting range of a gaussian fit to the measured energy spectra around a given K-line (Fig. 3 left). Resolution of the K-lines of carbon ranges between 25 % and 40 % depending on the detector unit (acceptable considering the low energy region and it is similar to the low energy prompt ones).

6. Data analysis

The detection of delayed X-rays is the signature of the muon transfer process. Events where the baseline RMS exceeds 20 ADC counts and the waveform saturates, hence not the whole energy of the waveform is collected, are discarded. Two pulses should be separated by at least 30 ns to suppress the pile-up. To evaluate the rate of muon transfers, the number of delayed X-rays is taken in a time window sufficiently separated from the prompt region and divided into ten logarithmic time interval bins. A different binning lead to a difference in the transfer rate extraction of 3.5 %.

Efficiency is always higher than 95 % as it is shown in Fig. 4 while live time is always higher than 99 %. The H_2 and H_2/CH_4 energy spectra are normalized between 200 and 400 keV and subtracted. X-rays from the transfer rate to carbon are calculated between 50 and 100 keV. The main source of background is bremsstrahlung radiation from electrons emitted in the muon decays. Signal is well visible confirming the high performances of the detecting system.

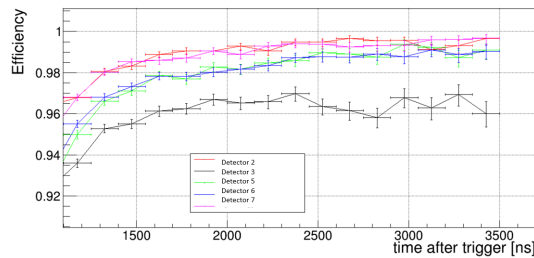


Figure 4: Efficiency in the delayed region for the 5 best performing scintillating detectors.

7. The Carbon transfer rate

At a temperature T , the number of μp ($N_{\mu p}$) changes with the time t according to the formulas:

$$dN_{\mu p}(t) = -N_{\mu p}(t)\lambda_{dis}(T)dt \quad (1)$$

$$\lambda_{dis}(T) = \lambda_0 + \phi[c_p\Lambda_{pp\mu} + c_d\Lambda_{pd}(T) + c_C\Lambda_{pC}(T)] \quad (2)$$

where $\lambda_{dis}(T)$ is the total disappearance rate of μp , λ_0 is the disappearance rate of the muons, $\Lambda_{pp\mu}$ is the $pp\mu$ formation rate, Λ_{pd} is the muon transfer rate from μp to deuterium, Λ_{pC} is the muon transfer rate from μp to carbon, ϕ is the atom density in the target, c_p , c_d and c_C are the hydrogen, deuterium and carbon atomic concentrations in the target. Λ_{pC} is extracted by counting the X-rays from carbon in the 10 logarithmic bins as it has been described previously.

Consistency check shows that the optimal choice of the starting time is 1500 ns when the rate of prompt X-rays becomes negligible. Instead the number of X-rays for $t_s > 4000$ ns is too low.

8. Conclusions

The first measurement of the muon transfer rate to carbon in the temperature range of 197-300 K was based on $\text{LaBr}_3(\text{Ce})$ scintillating crystals. $\text{LaBr}_3(\text{Ce})$ have a rise and decay times up to respectively 10 and 30 ns, with a resolution of the K-lines of carbon between 25 % and 40 % and very efficient (higher than 95 %). This let to discriminate the X-rays coming from the K-lines of carbon from background. New data-taking is on progress with laser with an improved detector system based on this technology. Besides the interest for the FAMU experiments, these measurements offer the possibility to develop future analysis on the muon transfer rate from hydrogen to heavier atoms.

9. Acknowledgements

The research has been carried out in the FAMU experiment funded by Istituto Nazionale di Fisica Nucleare (INFN). We thank RAL and the RIKEN-RAL facility the help in the set-up of the experiment, the Criotec company for the construction of the target. D.B., P.D. and M.S. acknowledge the support from Grant DN 08-17 of the Bulgarian Science Fund.

References

- [1] A. Antognini, *et al.* "The Proton Structure in and out of Muonic Hydrogen", Annual review of nuclear and particle science, 389-418, 2022, doi = 10.1146/annurev-nucl-101920-024709
- [2] E. Mocchiutti *et al.* "The FAMU experiment: muonic hydrogen high precision spectroscopy studies", Eur. Phys. J. A, 56, 2020, doi = 10.1140/epja/s10050-020-00195-9
- [3] T. Matsuzaki *et al.* "The RIKEN-RAL pulsed muon facility", Nucl. Instr. Meth. A, 465, 2001, doi = 10.1016/S0168-9002(01)00694-5
- [4] A. Adamczak *et al.* "The FAMU experiment at RIKEN-RAL to study the muon transfer rate from hydrogen to other gases", JINST 13, P12033, 2018, doi = 10.1088/1748-0221/13/12/P12033